# Early stages of surface graphitization on nanodiamond probed by x-ray photoelectron spectroscopy

Tristan Petit,[1,*] Jean-Charles Arnault,[1] Hugues A. Girard,[1] Mohamed Sennour,[2] and Philippe Bergonzo[1]
[1]*CEA, LIST, Diamond Sensors Laboratory, F-91191 Gif-sur-Yvette, France*
[2]*Mines Paris, Paristech CNRS UMR 7633, Boîte Postale 87, F-91003 Evry Cedex, France*
(Received 15 September 2011; revised manuscript received 14 November 2011; published 19 December 2011)

We have investigated the early stages of graphitization on detonation nanodiamond during sequential annealing treatments under vacuum using x-ray photoelectron spectroscopy. Two different temperature-dependent regimes were observed. Below 900 °C, the nanodiamond surface reconstructs into graphitic domain but does not alter the diamond core. Above 900 °C, graphitization, i.e., carbon hybridization changes from $sp^3$ to $sp^2$, occurs from the nanodiamond surface toward the diamond core. Graphitization is observed at much lower temperatures on nanodiamonds than on bulk diamond due to the high concentration of structural defects on their surface. These results indicate that low-temperature annealing under vacuum is an efficient method to uncouple surface and bulk graphitization. Hybrid nanocarbons formed in these conditions, constituted of a diamond core with a thin graphitic outer shell, may have interesting catalytic and chemical properties.

DOI: 10.1103/PhysRevB.84.233407 PACS number(s): 68.35.bt, 64.70.Nd, 61.46.Df

Nanodiamonds (NDs) are promising candidates as metal-free catalysts,[1,2] or as biomarkers[3,4] and drug delivery vectors[5,6] for biomedical applications. Indeed, NDs combine intrinsic properties of nanomaterials, including small sizes and high surface-to-volume ratios, with unique diamond properties such as high thermal stability[7] and the existence of photostable color centers[8] associated with a controllable surface reactivity.[9] In particular, remarkable chemical[10,11] and catalytic[1] properties have recently been reported on NDs annealed under vacuum below 900 °C. Enhanced reactivity was attributed to the formation of $sp^2$ carbon on the ND surface.[1,10] Nevertheless, the corresponding graphitic structures could hardly be detected around the diamond core using high-resolution transmission electron microscopy (HRTEM).[1,10] Although it is now well established that onionlike carbon is formed by graphitization of NDs after annealing under vacuum at temperatures above 1000 °C,[7,12,13] surface transformations occurring at lower temperatures still remain poorly understood.

In this study, we investigate the early stages of graphitization on detonation NDs during successive annealing treatments under ultrahigh vacuum (UHV) using x-ray photoelectron spectroscopy (XPS). NDs, provided by the NanoCarbon Research Institute Co., Ltd. (Japan), were exposed to annealing treatments at 700, 900, and 1100 °C while maintaining the pressure below $5 \times 10^{-9}$ mbar. For UHV analysis, NDs dispersed in water were deposited by drop casting on a multilayer silicon on insulator substrate with a 10-nm-thick silicon nitride overlayer because earlier studies had demonstrated that NDs exhibit a high thermal stability on silicon nitride substrates.[14] The surface chemistry evolution was monitored by XPS between each annealing at pressures below $5 \times 10^{-10}$ mbar, using a monochromatized Al $K\alpha$ anode (1486.6 eV), calibrated versus the Au $4f_{7/2}$ peak located at 84.0 eV. The spectrometer was equipped with an EA 125 hemispherical analyzer. The pass energy was 20 eV, corresponding to an energy absolute resolution of 0.6 eV. All experiments are conducted without air exposure since NDs are strongly sensitive to surface contamination. In a previous study, we showed that this experimental approach appears particularly powerful to characterize the hydrogenation of NDs under a chemical-vapor deposition (CVD) plasma.[15]

XPS is a well-known surface technique which probes several nanometers under the sample surface. It has been recently shown that the surface signal of nanoparticles on XPS spectra was strongly enhanced when their radius approaches the photoelectron escape path length.[16] For carbon materials, the inelastic mean-free path of C 1$s$ photoelectrons remains below 3 nm, close to the radius of detonation NDs.[17] In that case, the whole volume of the nanoparticles is probed, which results in a significant increase of the signal from the outer atomic layers compared to that probed on bulk material. Several studies have shown that XPS is highly sensitive to carbon hybridization changes at the diamond surface after annealing treatments.[18–21] Using this experimental approach, we will show that different surface transformations may occur according to the annealing temperature. Furthermore, we will discuss the graphitization mechanisms on NDs and their particularity with respect to that observed on bulk diamond, as induced by the presence of surface defects.

The size and morphology of the initial NDs were investigated using HRTEM using a FEI Tecnai F20 field-emission gun microscope operating at 200 kV [Fig. 1(a)]. Images were performed near Scherzer focalization (−63 nm) using a (1 k × 1 k) charge-coupled device camera. Local area fast Fourier transform diffractograms, equivalent to electron diffraction patterns, were exploited in order to determine structural and crystallographic characteristics of the observed NDs. The NDs present a size distribution of 6 ± 1 nm. Their diamond core exhibits the interplane distance of 2.06 Å corresponding to (111) diamond planes, surrounded by a disordered carbon shell of less than 1 nm. The XPS spectrum of initial NDs, shown on Fig. 1(b), consists mainly of an intense carbon peak and weak contributions assigned to nitrogen and oxygen. The detection limit of our XPS setup is of 0.5 at. % and no signal from the silicon nitride substrate could be detected. Nitrogen is commonly found in NDs synthesized with nitrogen-containing explosives[22,23] while different carbon/oxygen bonds are usually observed on their surface after purification treatments.[24] Areas of carbon, oxygen, and

 

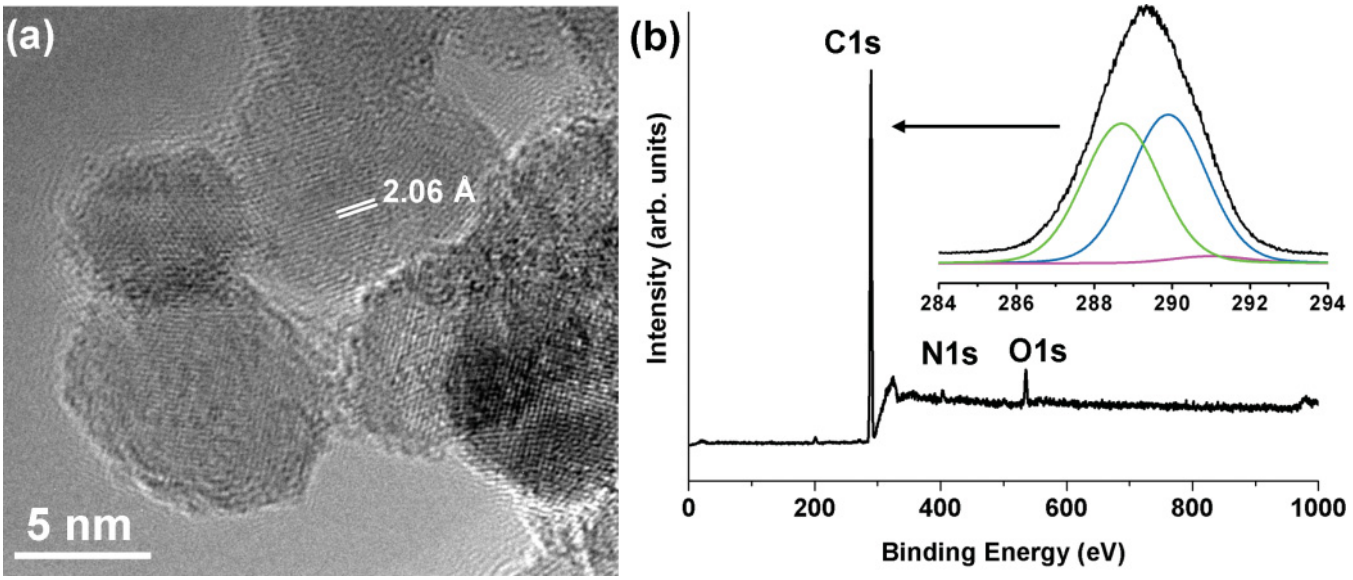


FIG. 1. (Color online) (a) HRTEM image and (b) XPS spectra of initial detonation NDs. Inset shows the C 1*s* carbon core level plotted above the related fitting components.

nitrogen core levels were extracted from XPS spectra after a Shirley background correction. The oxygen and nitrogen atomic concentrations are estimated to be 3.8 and 4.0 ± 0.5 at. %, respectively, taking into account the photoionization cross sections. The carbon core level (C 1*s*) XPS spectrum was fitted using Voigt functions with a Lorentzian width of 0.4 eV. The C 1*s* peak shows a broad peak at 289.0 eV exhibiting a full width at half maximum (FWHM) of 2.9 eV. Three peaks located at 288.7, 289.9, and 291.0 eV with FWHM of 2.3 eV were used to fit the C 1*s* peak.

The first peak at 288.7 eV is mainly attributed to $sp^3$-hybridized carbon. C-H bonds, already observed on raw NDs,[25] may also contribute to this peak. It is strongly shifted and broadened compared to that of bulk polycrystalline diamond reference, located at 285.0 eV and exhibiting a FWHM of 0.8 eV.[15] The energy shift and the peak broadening are mostly affected by charging effects resulting from the insulating properties of the thick ND layer. The two other peaks are partly related to carbon atoms bonded to different functional groups. The peak located at +1.2 eV from the $sp^3$ carbon peak could be attributed to single C-O bonds[26] and/or single C-N bonds.[27] The peak area represents 50 ± 2% of the total C 1*s* peak area, which is not compatible with the measured total oxygen and nitrogen atomic concentrations, implying that another contribution has to be considered. We suggest that structural defects on NDs may also contribute to this peak. In fact, on bulk diamond surfaces, the formation of defects after ion irradiation with $Ar^+$ or $N_2^+$ ions induces an additional broad peak at the C 1*s* core level, upshifted of 0.9 and 1.2 eV from the $sp^3$ peak, respectively.[27] This energy shift is attributed to a band bending at the valence band induced by defects created in the vicinity of the surface. Defects could have different origins on detonation NDs. In the bulk, defects such as twinning between NDs can lead to a highly stressed region where nitrogen-vacancy defects accumulate.[22,28] Additionally, unpaired electrons within the outer shells of the ND were measured by electron paramagnetic resonance[25,29,30] or by x-ray fluorescence spectroscopy.[31] Such unpaired electrons could originate from the disordered outer carbon shell observed by HRTEM [Fig. 1(a)]. Finally, the third peak at +2.3 eV is assigned to double C = O bonds.[15] The peak area corresponds to 3.4 ± 2% of the total carbon peak area. These results are in agreement with the nonaromatic core-shell structure of detonation NDs as recently reported, where the diamond core is surrounded by a disordered shell of $sp^3$-hybridized carbon, mainly protonated or bonded to OH groups.[25] Note that no $sp^2$-hybridized carbon is detected by XPS at this stage on the ND surface.

After 1 h annealing at 700 °C, the oxygen concentration drops drastically and traces close to the XPS detection limit (0.5 at. %) could be extracted from the background. Consequently, charging effects disappear leading to a downshift of

TABLE I. C 1*s* spectra fitting parameters as extracted from XPS measurements.

| Peak name | Peak attribution | | 700 °C | 900 °C | 1100 °C |
|---|---|---|---|---|---|
| CI | $sp^2$ | Binding energy (eV) | 284.5 | 284.4 | 284.3 |
| | | FWHM (eV) | 1.3 | 1.3 | 1.2 |
| CII | $sp^3$ | Binding energy (eV) | 285.9 | 285.8 | 285.7 |
| | | FWHM (eV) | 1.3 | 1.3 | 1.3 |
| CIII | Defects/C-N bonds | Binding energy (eV) | 286.9 | 286.9 | 286.9 |
| | | FWHM (eV) | 1.8 | 1.8 | 1.8 |

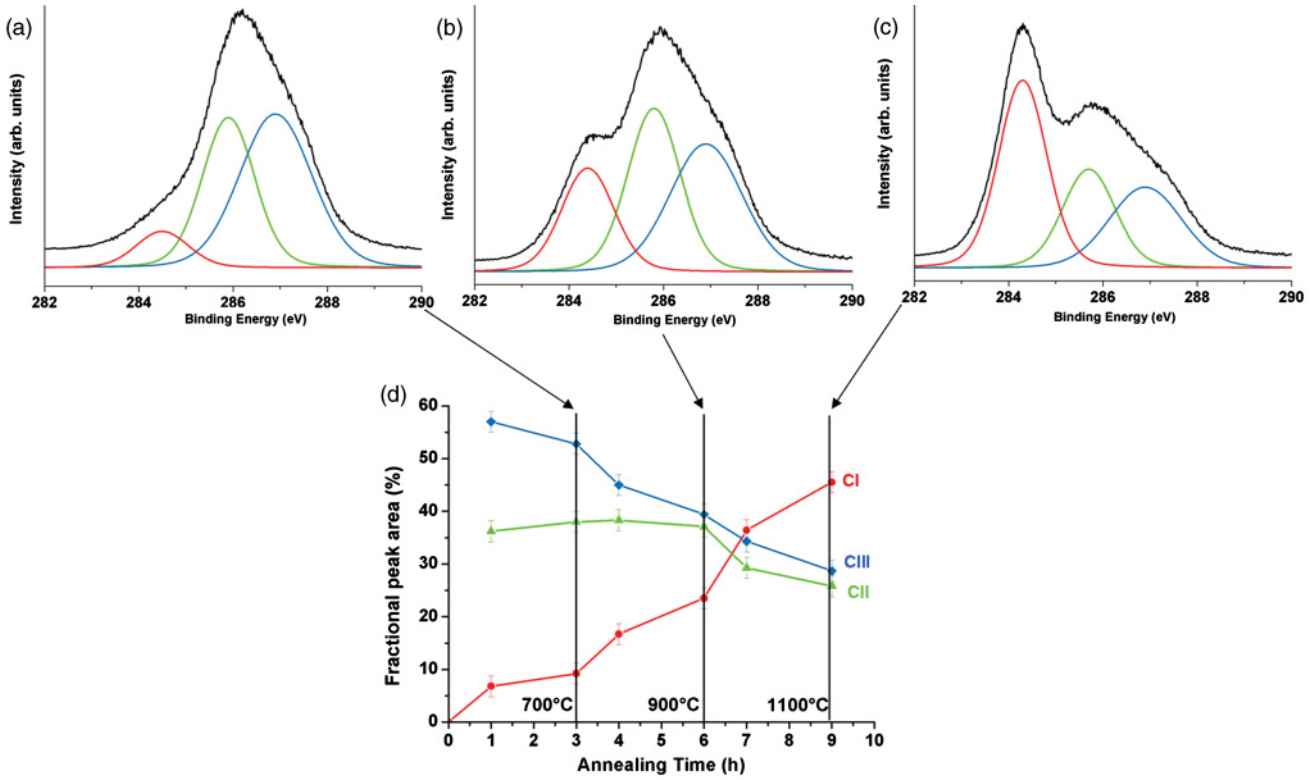


FIG. 2. (Color online) C 1*s* XPS spectra of NDs after sequential annealing treatments of 3 h at (a) 700, (b) 900, and (c) 1100 °C. Fitting components CI (red), CII (green), and CIII (blue), related to $sp^2$ carbon-carbon bonds, $sp^3$ carbon-carbon bonds, and defects, respectively, are plotted under the experimental curves. (d) Evolution of the fractional peak areas with respect to annealing time. Error bars result from experimental uncertainties on the relative peak areas extracted from fitting procedures.

the C 1*s* peak to 286.0 eV and a reduction of its FWHM to 2.1 eV. Three peaks located at 284.5, 285.9, and 286.9 eV, named, respectively, CI, CII, and CIII, are still required to fit the carbon core level efficiently. Parameters optimized to best fit the spectra are summarized in Table I. The C 1*s* spectrum obtained after 3 h at 700 °C is shown in Fig. 2(a).

CI and CII are assigned to $sp^2$- and $sp^3$-hybridized carbon, respectively. Energy upshifts of +0.4 and +0.9 eV are observed between CI and CII compared to our highly oriented pyrolytic graphite and polycrystalline diamond references, respectively. The FWHM of CI and CII is 1.3 eV, a value which is also above the FWHM measured on bulk materials (0.8 eV). Since charging effects cannot be imputed to oxygen which has been desorbed, the higher binding energies compared to bulk materials and the peak broadening are likely to result from the nanosize of the NDs.[16]

The attribution of CIII is more complicated as no similar peak is observed after UHV annealing of bulk diamond.[18,19] Indeed, these studies were significantly different as carried out on bulk diamond single crystals. Moreover, the surface was initially hydrogenated. Contributions at this binding energy are usually attributed to a chemical shift of $sp^3$ carbon due to the proximity of surface functional groups. However, single C-O bonds are in the present case excluded as no oxygen is detected and C-N bonds would not result in such an intense peak as the nitrogen atomic concentration remains low after annealing. Furthermore, charging effects are absent as the binding energy of CIII remains unmodified during all the annealing treatments (Table I). Therefore only the contribution of structural defects can explain the presence of CIII. In our experiments, energy differences between +1.0 and +1.2 eV are measured between CII and CIII, and thus are similar to the upshift observed on bulk diamond.[27] In addition to the defects initially observed on the ND surface, dangling bonds resulting from desorption of surface functional groups after annealing should also be considered. Dangling bonds are energetically unfavorable but since no hetero atoms can interact with the surface under UHV, they remain in a metastable state. As an example, on hydrogenated bulk (111) single-crystal diamond surfaces, an intermediate phase with a dangling-bond concentration reaching 70% could be observed after annealing at 730 °C under vacuum.[19] In that case, longer annealing times or higher annealing temperatures would both lead to the reconstruction into a hydrogen-free (2 × 1) surface once the critical dangling-bond concentration is reached.

Sequential annealing treatments above 700 °C were performed to investigate the role of the temperature on graphitization mechanisms on NDs. C 1*s* XPS spectra obtained after 3 h at 900 and 1100 °C, when fitted with similar parameters, are plotted in Figs. 2(b) and 2(c), respectively. The increase of CI with respect to temperature and annealing time shows that the $sp^2$ carbon is progressively formed and represents up to 45 ± 2% of the fractional peak area. Furthermore, the evolution of the fractional areas of CI, CII, and CIII, as plotted in Fig. 2(d), reveals that the $sp^2$ carbon formation rate increases with temperature. In addition, different surface

transformation mechanisms occur below and above 900 °C. Below 900 °C, the relative area of CII remains constant while CI increases and CIII decreases. Well-ordered $sp^3$-hybridized carbon atoms from the diamond core (CII component) are not altered in this temperature range while surface transformations involving surface defects (CIII component) are observed. More precisely, surface reconstructions occur that correspond to the conversion of the defective ND surface into graphitic domains involving $\pi$ bonds. A similar surface evolution has been reported on tetrahedral amorphous carbon.[32] Unpaired electrons from dangling bonds tend to form stable $\pi$ bonds with other unpaired electrons to reduce the total surface energy. This observation confirms simulation studies, demonstrating that fullerene-like reconstructions are spontaneously formed at the surface of NDs free of functional groups at low temperature.[33,34] After annealing at 1100 °C, the CII relative area starts to decrease, showing that the phase transition of the diamond core from $sp^3$ to $sp^2$ hybridization is initiated. The CIII area decays at a similar rate, which is in agreement with the dangling-bond-induced graphitization model as recently proposed by Li and Zhao.[35] Based on density functional theory computations, they demonstrated that graphitization on NDs is induced by dangling bonds at the diamond-graphite interface, leading to the rupture of carbon-carbon bonds between the two outer (111) diamond layers. According to this model, the carbon phase transformation from $sp^3$ to $sp^2$ hybridization saturates dangling bonds on the top carbon layer and results in the formation of new dangling bonds on the sublayer surface. As a consequence, the dangling-bond concentration at the ND surface is reduced but does not vanish during the graphitization process.

In conclusion, we have monitored the early stages of surface graphitization of detonation NDs during annealing under UHV using XPS sequential analysis. Two main transformations occur at the ND surface depending on the annealing temperature: (i) below 900 °C, the ND surface reconstructs into graphitic domains without altering the diamond core; (ii) above 900 °C, the diamond core is progressively graphitized. This graphitization mechanism strongly differs from that of bulk diamond, which is known to graphitize above 1600 °C.[7] This difference is mainly due to the high concentration of structural defects on the ND surface. These defects are either created during the detonation synthesis or result from desorption of the surface functional groups, and increase the reactivity of surface carbon atoms. These observations give insights to explain and control the unique surface reactivity of detonation NDs,[36] however it has to be noted that the graphitization kinetics depend strongly on the initial surface chemistry of the NDs. In particular, the higher-temperature desorption of C=O bonds may limit surface reconstruction on strongly oxidized NDs below 900 °C.[14] The selective synthesis of a thin graphitic layer on the ND surface by annealing under vacuum at relatively low temperatures (<900 °C), gives rise to hybrid nanocarbons which may combine the intrinsic core properties of diamond with the surface reactivity of $sp^2$-based nanomaterials.

*tristan.petit@cea.fr


[1] J. Zhang, D. S. Su, R. Blume, R. Schlögl, R. Wang, X. Yang, and A. Gajović, Angew. Chem., Int. Ed. **49**, 8640 (2010).

[2] D. Yu, E. Nagelli, F. Du, and L. Dai, J. Phys. Chem. Lett. **1**, 2165 (2010).

[3] Y.-R. Chang, H.-Y. Lee, K. Chen, C.-C. Chang, D.-S. Tsai, C.-C. Fu, T.-S. Lim, Y.-K. Tzeng, C.-Y. Fang, C.-C. Han, H.-C. Chang, and W. Fann, Nat. Nanotechnol. **3**, 284 (2008).

[4] L. P. McGuinness, Y. Yan, A. Stacey, D. A. Simpson, L. T. Hall, D. Maclaurin, S. Prawer, P. Mulvaney, J. Wrachtrup, F. Caruso, R. E. Scholten, and L. C. L. Hollenberg, Nat. Nanotechnol. **6**, 358 (2011).

[5] M. Chen, X.-Q. Zhang, H. B. Man, R. Lam, E. K. Chow, and D. Ho, J. Phys. Chem. Lett. **1**, 3167 (2010).

[6] E. K. Chow, X.-Q. Zhang, M. Chen, R. Lam, E. Robinson, H. Huang, D. Schaffer, E. Osawa, A. Goga, and D. Ho, Sci. Transl. Med. **3**, 73ra21 (2011).

[7] Y. V. Butenko, V. L. Kuznetsov, A. L. Chuvilin, V. N. Kolomiichuk, S. V. Stankus, R. A. Khairulin, and B. Segall, J. Appl. Phys. **88**, 4380 (2000).

[8] C. Bradac, T. Gaebel, N. Naidoo, M. J. Sellars, J. Twamley, L. J. Brown, A. S. Barnard, T. Plakhotnik, A. V. Zvyagin, and J. R. Rabeau, Nat. Nanotechnol. **5**, 345 (2010).

[9] A. Krueger, J. Mater. Chem. **18**, 1485 (2008).

[10] T. Meinhardt, D. Lang, H. Dill, and A. Krueger, Adv. Funct. Mater. **21**, 494 (2011).

[11] G. Jarre, Y. Liang, P. Betz, D. Lang, and A. Krueger, Chem. Commun. **47**, 544 (2011).

[12] V. L. Kuznetsov, I. L. Zilberberg, Y. V. Butenko, A. L. Chuvilin, and B. Segall, J. Appl. Phys. **86**, 863 (1999).

[13] O. O. Mykhaylyk, Y. M. Solonin, D. N. Batchelder, and R. Brydson, J. Appl. Phys. **97**, 074302 (2005).

[14] S. Zeppilli, J. C. Arnault, C. Gesset, P. Bergonzo, and R. Polini, Diamond Relat. Mater. **19**, 846 (2010).

[15] J.-C. Arnault, T. Petit, H. Girard, A. Chavanne, C. Gesset, M. Sennour, and M. Chaigneau, Phys. Chem. Chem. Phys. **13**, 11481 (2011).

[16] D. R. Baer and M. H. Engelhard, J. Electron Spectrosc. Relat. Phenom. **178-179**, 415 (2010).

[17] S. Tanuma, C. J. Powell, and D. R. Penn, Surf. Interface Anal. **37**, 1 (2005).

[18] R. Graupner, F. Maier, J. Ristein, L. Ley, and C. Jung, Phys. Rev. B **57**, 12397 (1998).

[19] J. B. Cui, J. Ristein, and L. Ley, Phys. Rev. B **59**, 5847 (1999).

[20] Y. V. Butenko, S. Krishnamurthy, A. K. Chakraborty, V. L. Kuznetsov, V. R. Dhanak, M. R. C. Hunt, and L. Šiller, Phys. Rev. B **71**, 075420 (2005).

[21] M. Yeganeh, P. R. Coxon, A. C. Brieva, V. R. Dhanak, L. Šiller, and Y. V. Butenko, Phys. Rev. B **75**, 155404 (2007).

[22] I. I. Vlasov, O. Shenderova, S. Turner, O. I. Lebedev, A. A. Basov, I. Sildos, M. Rähn, A. A. Shiryaev, and G. Van Tendeloo, Small **6**, 687 (2010).

[23] V. Pichot, O. Stephan, M. Comet, E. Fousson, J. Mory, K. March, and D. Spitzer, J. Phys. Chem. C **114**, 10082 (2010).

[24] V. Pichot, Diamond Relat. Mater. **17**, 13 (2008).

[25] X. Fang, J. Mao, E. M. Levin, and K. Schmidt-Rohr, J. Am. Chem. Soc. **131**, 1426 (2009).
[26] S. Ferro, M. Dal Colle, and A. De Battisti, Carbon **43**, 1191 (2005).
[27] I. Kusunoki, M. Sakai, Y. Igari, S. Ishidzuka, T. Takami, T. Takaoka, M. Nishitani-Gamo, and T. Ando, Surf. Sci. **492**, 315 (2001).
[28] S. Turner, O. I. Lebedev, O. Shenderova, I. I. Vlasov, J. Verbeeck, and G. Van Tendeloo, Adv. Funct. Mater. **19**, 2116 (2009).
[29] A. I. Shames, A. M. Panich, W. Kempinski, A. E. Alexenskii, M. V. Baidakova, A. T. Dideikin, V. Y. Osipov, V. I. Siklitski, E. Osawa, M. Ozawa, and A. Y. VuÍ, J. Phys. Chem. Solids **63**, 1993 (2002).
[30] A. V. Fionov, A. Lund, W. M. Chen, N. N. Rozhkova, I. A. Buyanova, G. I. Emel'yanova, L. E. Gorlenko, E. V. Golubina, E. S. Lokteva, and E. Ōsawa, Chem. Phys. Lett. **493**, 319 (2010).
[31] A. V. Okotrub, L. G. Bulusheva, V. L. Kuznetsov, A. V. Gusel'nikov, and A. L. Chuvilin, Appl. Phys. A **81**, 393 (2004).
[32] W. Conway, N. M. J. Ferrari, A. C. Flewitt, A. Robertson, J. J. Milnea, W. I. Tagliaferrob, and A. Beyerc, Diamond Relat. Mater. **9**, 765 (2000).
[33] J.-Y. Raty, G. Galli, C. Bostedt, T. W. van Buuren, and L. J. Terminello, Phys. Rev. Lett. **90**, 037401 (2003).
[34] A. Sorkin, B. Tay, and H. Su, J. Phys. Chem. A **115**, 8327 (2011).
[35] L.-sheng Li and X. Zhao, J. Chem. Phys. **134**, 044711 (2011).
[36] O. A. Williams, J. Hees, C. Dieker, W. Jäger, L. Kirste, and C. E. Nebel, ACS Nano **4**, 4824 (2010).